Morphology and Thermal Stability of Metal Contacts on Crystalline Organic Thin Films**

By *Arndt C. Dürr*, *Frank Schreiber*,* *Marion Kelsch*, *Heinz D. Carstanjen*, and *Helmut Dosch*

Due to their potential in electronic and optoelectronic applications, semiconducting organic materials are the focus of a rapidly increasing research activity. Organic field-effect transistors, organic light-emitting diodes, or organic solar cells are only a few examples of tailored organic device structures.[1] Besides high charge-carrier mobilities in the organic layer, the proper function of the contact between the metal and the organic layer is of great importance for the device performance. Thus, knowledge of the associated morphology of the metal–organic interface as well as its thermal stability is essential. Hitherto, only a few studies of metal–organic interfaces exist, mostly on disordered polymers used as low dielectric constant material in conventional microelectronic fabrication processes[2] and some on Langmuir–Blodgett films[3] and on ultra-high vacuum (UHV)-deposited organic thin films.[4]

In this paper, we present a study of the interface between gold and diindenoperylene thin films (DIP, $C_{32}H_{16}$, Fig. 1C) as a model system for metal contacts on organic electronic devices. We examine the necessary preparation conditions that lead to a well-defined gold/DIP interface in the as-grown state by cross-sectional TEM and study the thermal stability of the DIP thin film at elevated temperatures by in-situ X-ray-scattering. Finally, we investigate the thermal stability of the metal–organic interface employing in-situ, high-resolution Rutherford backscattering spectrometry (RBS) as a function of temperature. The annealing studies are particularly important to address the issue of thermal stability of devices operating at elevated temperatures.

DIP was chosen as the organic material, since the surface of the DIP films exhibits large terraces (up to 7000 Å) with monomolecular steps of 16.5 Å. Thus, DIP films are very well defined and ideally suited for the study of the interfacial structure of metal contacts on organic thin films. Moreover, DIP exhibits excellent crystalline order and very good charge-transport properties associated with it.[5] Gold is widely used for contacting organic electronic devices and rather inert, hence, specific chemical interactions play only a minor role. This allows us to focus on the role of substrate temperature and deposition rate on the morphology of the metal–organic interface.

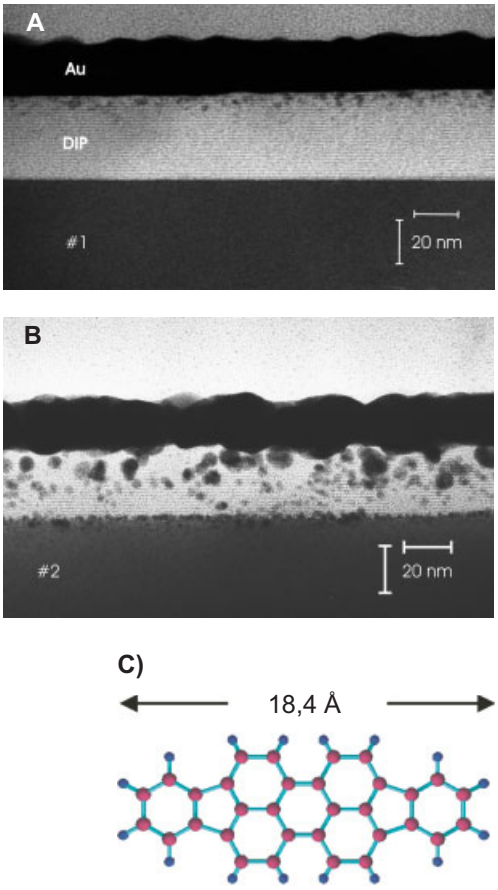

Fig. 1. A) Cross-sectional TEM of sample 1. B) Cross-sectional TEM of sample 2. C) Structure of diindenoperylene (DIP, $C_{32}H_{16}$).

Based on a comparison with previous experiments and Monte Carlo simulations of metals on polymers,[2,6] one may expect the largest differences in interfacial morphology for metal deposition on crystalline organic films in the as-grown state for the two following extreme growth conditions:

- low substrate temperature combined with a high deposition rate
- high substrate temperature combined with a small deposition rate

Although there are important differences between disordered polymer films and crystalline films of comparatively small molecules regarding the diffusion channels of metals into these films, we use these extreme cases as a starting point.

Therefore, we prepared two samples (denoted as sample 1 and 2; see Table 1) under the above mentioned different growth conditions to investigate the interfacial morphology in

Table 1. Preparation conditions of the gold layer on top of the DIP film.

Sample	T_{Sub} [°C]	Rate [Å min^{-1}]	Thickness [Å]
1	–120	23	135
2	+70	0.35	135
3	+25	1	70

[*] Dr. F. Schreiber,[+] A. C. Dürr, M. Kelsch, Dr. H. D. Carstanjen, Dr. H. Dosch
Max-Planck-Institut für Metallforschung
Heisenbergstrasse 1, D-70569 Stuttgart (Germany)
Dr. F. Schreiber, A. C. Dürr, Dr. H. D. Carstanjen, Dr. H. Dosch
Institut für Theoretische und Angewandte Physik, Universität Stuttgart
Pfaffenwaldring 57, D-70550 Stuttgart (Germany)
[+] Present address: Physical and Theoretical Chemistry, University of Oxford, South Parks Road, Oxford, OX1 3QZ, UK.
E-mail: fschreib@physchem.ox.ac.uk.

[**] We gratefully acknowledge D. Plachke for help during the RBS measurements, O. H. Seeck for support at beamline W1 at HASYLAB, and N. Karl for fruitful discussions. The authors acknowledge partial support from the DFG (focus program "Organische Feldeffekt-Transistoren").

  0935-9648/02/1307-0961 $ 17.50+.50/0

ADVANCED MATERIALS

the as-grown state by cross-sectional TEM. Furthermore, sample 1 was used for X-ray studies during annealing. The thermal stability of the gold/DIP interface as probed by RBS will be discussed using sample 3.[7] In addition to the samples discussed here, others were studied in complementary experiments, confirming the conclusions presented in this paper.

The TEM images of sample 1 and 2 (Fig. 1A and 1B) show the gold layer on top of the crystalline DIP layer. Remarkably, one clearly observes individual molecular lattice planes of the DIP film, where each pair of horizontal stripes with bright–dark contrast is associated with one monolayer of the essentially upright standing DIP molecules. This shows the excellent crystalline order of the DIP film across the entire thickness (at the bottom the SiO_2 substrate is seen).

As is obvious from the images the interfacial morphology is very different for both samples. Sample 1 exhibits a well-defined gold/DIP interface with only a few small gold clusters that have diffused into the topmost layers of the DIP film. Apparently, the low substrate temperature limits the diffusion of gold atoms into the DIP film. Furthermore, the high deposition rate increases the probability that an adsorbed gold atom forms a less mobile cluster with other gold atoms, which also contributes to limiting the diffusion.

Consistent with this, the combination of high substrate temperature and low rate for sample 2 leads to an almost complete intermixing of gold and DIP. Large gold clusters are embedded inside the DIP film and penetrate to the SiO_2/DIP interface. This study clearly shows that it is very important to choose appropriate preparation conditions to obtain well-defined and controlled metal–organic interfaces.

We now turn to the thermal stability of the organic layer and the degree of diffusion of metal into the organic layer under (simulated) elevated operation temperatures. For this purpose we performed temperature-dependent, in-situ X-ray diffraction measurements of sample 1. In addition, we carried out temperature-dependent RBS measurements of sample 3.

In Figures 2A–C we show the results of an X-ray study of the thermal stability of the DIP-layer in this heterostructure. Figures 2A and 2B show the DIP(001) reflection with its Laue-oscillations for sample 1 at different temperatures and the scattering geometry, respectively. In Figure 2A, the X-ray reflectivity data are also plotted for the sample in the as-grown state. The long wavelength oscillations around $q_z = 0.1$–0.2 Å^{-1} stem from the gold layer with a uniform thickness of about 135 Å on top of the DIP film. The Laue oscillations around the DIP(001) reflection again confirm the high structural order of the DIP film with a coherent thickness, d_{coh}, of about 385 Å, which is laterally uniform and which equals the total thickness of the DIP film.

During the annealing the DIP(001) reflection does not change significantly for $T \leq 150\,^{\circ}C$, as is shown in Figure 2A and Figure 2C, which display the integrated intensity of the reflection (shaded area in Figure 2A) as a function of temperature (filled circles in Figure 2C). Yet, a further increase of the temperature results in a significant decay of intensity of the DIP(001) reflection, which we associate with the desorption of DIP molecules (Fig. 2C, note the log scale of the *y*-axis). This implies that the DIP film is thermally stable up to $T = 150 \pm 10\,^{\circ}C$ under the annealing conditions employed (see Experimental), which is sufficient for typical device applications. In contrast to the integrated intensity, d_{coh} remains largely unchanged throughout the annealing (Fig. 2C). This means that the breakdown of the structure at still higher temperatures is obviously due to a laterally inhomogeneous process, leaving DIP islands of constant height, while major fractions of the film are already desorbed.

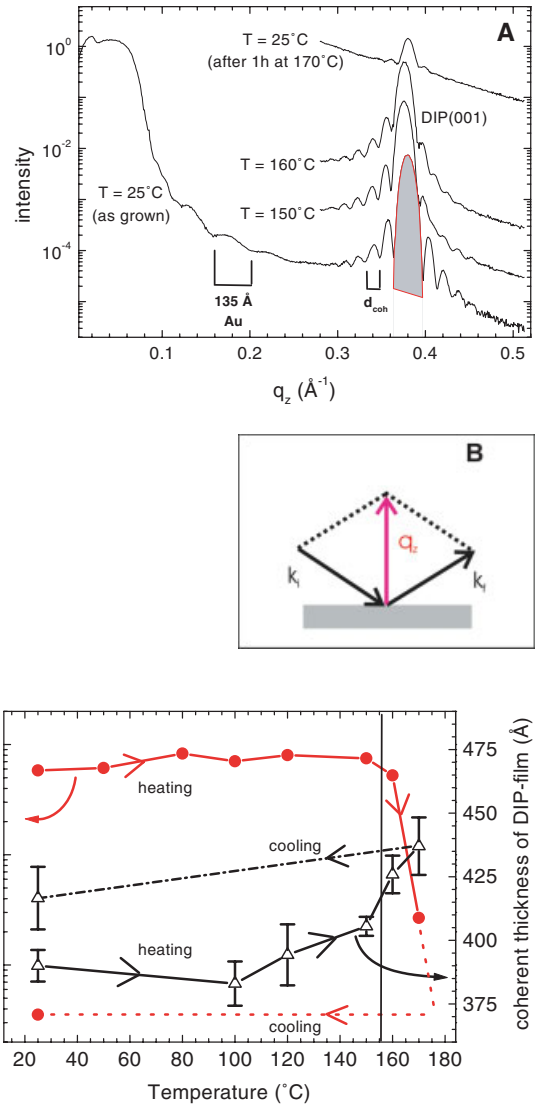

Fig. 2. A) DIP(001) reflection of sample 1 for different annealing temperatures. The different scans are offset to each other for clarity. For the sample in the as-grown state the X-ray-reflectivity data are also plotted. B) Schematic plot of the specular scattering geometry. C) Normalized intensity (filled circles) of the DIP(001) reflection (shaded area in A) and coherent thickness, d_{coh}, of the DIP-film (open triangles) as a function of the annealing temperature. The vertical line marks the upper temperature limit for stability of the DIP film.

Next, we turn to the thermal stability of the Au/DIP interface. For this purpose, we carried out in-situ, temperature-dependent, high energy resolution RBS measurements on sample 3. In Figure 3 the spline-fitted RBS gold peak is

  0935-9648/02/1307-0962 $ 17.50+.50/0

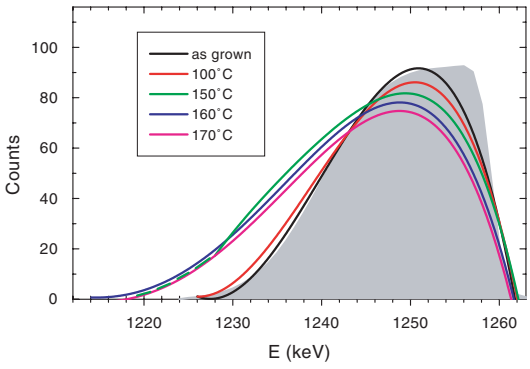

Fig. 3. RBS measurements around the gold edge of sample 3. The figure shows the spline-fitted RBS gold peak just after gold deposition (black), and after annealing at $T = 100\,^{\circ}C$ (red), 150 °C (green), 160 °C (blue), and 170 °C (magenta) for one hour each. The slightly rounded edges on the high-energy side are indicative of small amounts of adsorbed material on top of the gold film. For comparison, the gray shaded area shows an RBS simulation for an ideal Au film with 70 Å average thickness and 25 Å thickness fluctuation.

displayed, measured just after deposition and after annealing at different temperatures for one hour each. Immediately after deposition the gold peak exhibits a slightly smeared-out shape with relatively steep edges at the high- and low-energy side, pointing to an essentially homogeneous and well-defined film with only little interdiffusion. The simulation (gray area in Fig. 3) gives a film thickness of 70 Å and a thickness fluctuation of 25 Å. The latter equals the surface roughness of the DIP film as determined by X-ray reflectivity measurements.

Although for technical reasons sample 3 could not be prepared completely the same as sample 1, the RBS data provide evidence for a well-defined interface between the gold and the DIP layer. Annealing at 100 °C does not change the peak significantly, demonstrating that the interface is thermally stable against interdiffusion. Further annealing at 150 °C results in a noticeable change of the shape of the peak: the FWHM of the peak increases, and the low-energy side exhibits a longer tail. This is a clear sign for diffusion of gold into the DIP film. Remarkably, the peak shape does not change any more upon further annealing to 160 °C and 170 °C, which suggests that the gold diffusion process is completed already at 150 °C, most likely due to the formation of immobile gold clusters. However, at the two highest annealing temperatures, the position of the gold edge shifts to lower energies by ≈ 1 keV. This implies that the gold film is covered by a thin DIP film of about 15 Å in thickness, indicating that at this stage wetting effects play a role.

In conclusion, we have shown that the interfacial properties of metal contacts on organic materials in the system gold on DIP are strongly determined by the preparation conditions of the gold film. Gold deposition at a high rate (20 Å min^{-1}) and low substrate temperatures during deposition (–120 °C) leads to well-defined interfaces with only a slight amount of interdiffusion. Moreover, we found that the interface is stable against further interdiffusion up to 100 °C and that the DIP structure itself is stable even up to 150 °C. These temperatures are supposed to be sufficient for most technical applications of metal contacts on organic semiconductors.

Experimental

All samples were prepared on atomically smooth oxidized (4000 Å) Si(100) substrates. A DIP-layer of typically 400 Å in thickness was grown at $T_{Sub} = 145 \pm 5\,^{\circ}C$ and a rate R of 12 ± 3 Å min^{-1} under UHV conditions. The gold film was deposited after growth of the DIP film in the same chamber. The deposition conditions for the gold layer on top of the DIP film are shown in Table 1. For a detailed characterization of this multilayer structure, TEM images were taken by a JEOL FX4000 and a Philips CM200 microscope, at 400 kV and 200 kV, respectively. X-ray measurements were carried out at beamline W1 at HASYLAB with a wavelength of $\lambda = 1.39$ Å. The RBS data were taken at the Stuttgart Pelletron [8] with He^+ ions at 1.3 MeV and a scattering angle of $\theta = 75°$. We used a high energy resolution spectrometer with an energy resolution of $\Delta E = 2.4$ keV, corresponding to a depth resolution of ≈ 10 Å in gold. For the study of the thermal stability of the organic layer and the metal–organic interface as a function of temperature, the samples were mounted on a heater, annealed to a given temperature for one hour each, and measured in situ using X-ray-reflectivity and RBS, respectively, at each temperature step.

Received: January 14, 2002
Final version: April 16, 2002

[1] a) S. R. Forrest, *Chem. Rev.* **1997**, *97*, 1793. b) A. R. Brown, C. P. Jarrett, D. M. de Leeuw, M. Matters, *Synth. Met.* **1997**, *88*, 37. c) G. Horowitz, *Adv. Mater.* **1998**, *10*, 365. d) A. Ullmann, J. Ficker, W. Fix, H. Rost, W. Clemens, I. McCulloch, M. Giles, *Mater. Res. Soc. Symp. Proc.* **2001**, *665*, C7.5.1.

[2] a) F. Faupel, R. Willecke, A. Thran, *Mater. Sci. Eng. R* **1998**, *22*, 1. b) D. Gupta, F. Faupel, R. Willecke, in *Diffusion in Amorphous Materials* (Eds: H. Jain, D. Gupta), The Minerals and Materials Society, Warrendale, PA **1994**, p. 189. c) R. Tromp, F. LeGoues, P. Ho, *J. Vac. Sci. Technol. A* **1985**, *3*, 782.

[3] G. Philipp, C. Müller-Schwanneke, M. Burghard, S. Roth, K. v. Klitzing, *J. Appl. Phys.* **1999**, *85*, 3374.

[4] Y. Hirose, A. Kahn, V. Aristov, P. Soukiassian, V. Bulovic, S. R. Forrest, *Phys. Rev. B* **1996**, *54*, 13 748.

[5] a) A. C. Dürr, M. Münch, N. Karl, F. Schreiber, V. Kruppa, B. Krause, K. Ritley, H. Dosch, *Verhandlungen der DPG* **2001**, p. 371. b) A. C. Dürr, unpublished.

[6] a) F. K. LeGoues, B. D. Silverman, P. S. Ho, *J. Vac. Sci Technol. A* **1988**, *6*, 2200. b) B. Silverman, *Macromolecules* **1991**, *24*, 2467.

[7] For technical reasons it was not possible to exactly match the deposition conditions of sample 1, but the interfacial morphology of sample 3 is comparable to that of 1.

[8] H. D. Carstanjen, *Nucl. Instrum. Methods B* **1998**, *136–138*, 1183.

A Novel Conductive Polymer–Sulfur Composite Cathode Material for Rechargeable Lithium Batteries

By *Jiulin Wang*,* *Jun Yang*, *Jingying Xie*, and *Naixin Xu*

Demand is now increasing for rechargeable lithium batteries with a high energy density and long cycle life, as they have a wide application range—from microbatteries for small-size electronic devices, to power sources for electrical vehicles. The high energy density that is obtainable with a lithium battery is mainly due to the large charge density of the anode active materials such as lithium metal (3861 mAh g^{-1}) and lithium intercalation carbon materials (372 mAh g^{-1}). Therefore, the

[*] Dr. J. Wang, Prof. J. Yang, Prof. J. Xie, Prof. N. Xu
Energy Science and Technology Laboratory
Shanghai Institute of Microsystem and Information Technology
Chinese Academy of Sciences
Shanghai 200 050 (China)
E-mail: WJL1021@yahoo.com.cn

  0935-9648/02/1307-0963 $ 17.50+.50/0